Astron. Astrophys. 362, 273–280 (2000)

ASTRONOMY AND ASTROPHYSICS

IRAS 03201+5459: a C–rich AGB star with silicate absorption⋆

B.W. Jiang[1], **R. Szczerba**[2], **and S. Deguchi**[3]

[1] Beijing Astronomical Observatory, Chinese Academy of Sciences, Datun Rd. No.20(A), Beijing 100012, P.R. China
[2] N. Copernicus Astronomical Center, ul. Rabiańska 8, 87-100 Toruń, Poland
[3] Nobeyama Radio Observatory, Minamimaki, Minamisaku, Nagano 384–1305, Japan

Received 20 March 2000 / Accepted 17 August 2000

Abstract. IRAS 03201+5459 is a late–type star with a circumstellar envelope according to its IRAS color. It has no identification at optical or near–infrared wavelengths. A full ISO–SWS spectrum between 2.3 and 43 μm was taken at a resolution of about $\sim$300 to investigate its nature. The spectrum shows the 9.7 μm feature in absorption, usually seen in O–rich envelopes, and the 3 μm feature in absorption which is related to C–rich late–type stars. Furthermore, modeling of the spectral energy distribution indicates the necessity of C–based dust. To understand these conflicting spectral features, we have estimated interstellar extinction in the direction of IRAS 03201+5459 by different methods. In no case can we get a sufficiently large $A_{\rm V}$ to explain the observed strength of the 9.7 μm absorption feature as due to interstellar extinction. Therefore, we investigated the hypothesis that a central C–rich star is surrounded by an inner C–rich shell and an outer O–rich shell (the object may be in the transition stage of evolution from an O–rich to a C–rich star). However, this require a very short lifetime of the object as a C–rich star, and then the similarity between IRAS and ISO spectra makes this hypothesis difficult to sustain. Alternatively O–rich material around the C–star IRAS 03201+5459 might be confined into more stationary disk–like configuration which is seen (almost) edge–on.

Key words: stars: AGB and post-AGB – stars: chemically peculiar – stars: circumstellar matter – stars: individual: IRAS 03201+5459

1. Introduction

IRAS 03201+5459 (hereafter IRAS 03201) was first detected by the IRAS satellite (see The IRAS Point Source Catalogue) (PSC 1988). Fluxes at 12 and 25 microns, F_{12} and F_{25}, are 13.77 and 5.14 Jy, respectively, which are of good quality. The resulting color $C_{12} \equiv \lg(F_{25}/F_{12})$ is equal to -0.43 which is typical for a late–type star with a circumstellar envelope, possibly optically thin and warm if the star is located in region II, or cold if its IRAS 60 μm flux puts it in region VIa on the IRAS color–color diagram of van der Veen & Habing (1988). Due to the low quality of the IRAS flux at 60 μm (only upper limit values are available for the 60 and 100 μm fluxes) it is difficult to judge the properties of the object solely by its IRAS C_{12} color.

As the flux at 12 micron is relatively high, a Low Resolution Spectrum (LRS) between 7 and 23 μm was also obtained by IRAS. Based on a clear absorption feature around 10 μm it was classified as LRS 32 (Olnon et al. 1986). However, it is worth noting that Kwok et al. (1997) put this LRS spectrum into unusual (U) group according to a by eye classification scheme developed by Volk & Cohen (1989). It was assumed to be a carbon–rich source with silicate absorption due to interstellar extinction. This possibility will be discussed in more detail in Sect. 3.

After the discovery of this source during the IRAS mission, follow–up identification attempts were carried out, but no object from the existing catalogues was found to be associated with this source. An attempt at optical identification in POSS R plate gave a negative result (Jiang & Hu 1992), so the object is fainter than 21st magnitude in the R band. Moreover, there was no detection of the source in the near–infrared (IR) at the limit of magnitude 8 at K band, i.e. the flux at 2.2 μm is less than 0.4 Jy. The steep increase between the near–IR such as K band and the mid–IR (e.g. 12 μm) indicates strong emission in this range, for which an ISO Short Wavelength Spectrometer (SWS) observation was proposed. Searches for the molecular maser emissions from OH (Galt et al. 1989), H_2O (Zuckerman & Lo 1987) and SiO (Jiang et al. 1996) all failed. In consequence, no more measurements were available prior to the Infrared Space Observatory (ISO) observations aside from the IRAS photometry and spectroscopy.

2. Observation and data reduction

The spectroscopic observation was carried out with the SWS spectrometer (de Graauw et al. 1996) of the ISO satellite on July 31, 1997 with the second fastest speed covering full grating scan from 2.3 to 45 μm (SWS AOT 01, speed 2).

The Off Line Processing (OLP) version 8.6 data were corrected for dark current, up–down scan differences, flat–fielded

Send offprint requests to: B.W. Jiang (jiang@class1.bao.ac.cn)

⋆ Based on observations with ISO, an ESA project with instruments funded by ESA Member States (especially the PI countries: France, Germany, the Netherlands and the United Kingdom) and with participation of ISAS and NASA

and flux calibrated by using the Observers SWS Interactive Analysis (OSIA) package. The deglitching and averaging to equidistant spectral points in wavelengths across the scans and detectors was done by using the ISO Spectral Analysis Package (ISAP) package. The spectral resolution for the following analysis is taken to be 300.

The ISOCAM imaging was performed on July 31, 1997 with the CAM camera in mode AOT 01 with the LW3 filter centered at 15 μm. The data was reduced by using the ISOCAM Interactive Analysis (CIA) package. The source is point–like in the ISOCAM image. The flux through the filter LW3 measured by using the aperture photometry method is 14.38 Jy. Because of the photometric uncertainties and the waveband difference between the ISO–CAM LW3 and the IRAS 12 μm filters, the ISOCAM result is consistent with that of IRAS (13.77 Jy at 12 μm). This agreement shows that the object is probably not a large–amplitude variable, which is consistent with the variability index 29 from the IRAS photometry.

The spectra obtained from the OSIA analysis for band 3A, 3C and 3D (from 12.0 to 27.5 μm) are quite noisy and for further analysis only data from the best 6 to 7 detectors (out of 12) are used. The data for bands 3E and 4 (from 27.5 to 45.2 μm) are of poor quality and they are not taken into consideration. Among the reduced SWS data there are small discrepancies between consecutive bands. Namely, the flux levels of bands 2C, 3C and 3D are low in comparison with other bands. In order to correct for deficient flux (about 2 Jy) of band 2C, the spectrum in the same wavelength range as the photometric range of IRAS 12 μm filter is normalized to match with the photometric results from the IRAS PSC. The scaling factor of 1.15 applied to band 2C results in a correct simulated IRAS 12 μm flux and produces smoother transitions between neighbouring bands. At the same time, a factor of 1.245 was applied to the IRAS LRS spectrum in order to match with the IRAS photometric result at 12 μm. Since the SWS data beyond 27.5 micron are not reliable, the procedure of normalization to the IRAS 25 μm band flux cannot be applied. Therefore, bands 3C and 3D were scaled with respect to band 3A by multiplicative factors of 1.25 and 1.15 respectively, just to make the overall shape of the SWS spectrum smooth. Because the flux calibration of SWS observation has an uncertainty of 20–30 %, such corrections seem to be reasonable. The reliable part of the SWS spectrum (bands 1A–3D), after the flux adjustments described above, is displayed in Fig. 1 by a solid line. The dotted line represents the IRAS LRS spectrum multiplied by factor 1.245 and filled squares mark the IRAS PSC fluxes at 12 and 25 μm. As can be seen, the overall agreement between both sets of spectroscopic data is satisfactory.

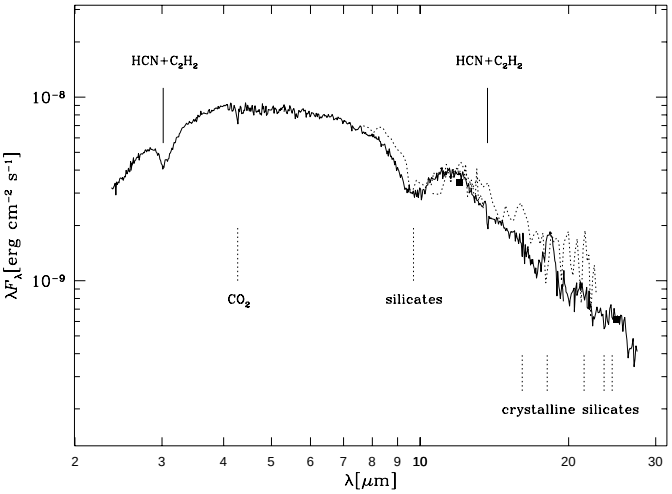

Fig. 1. The ISO–SWS spectrum of IRAS 03201+5459 (solid line) together with the IRAS LRS spectrum (dotted line) and the IRAS PSC photometric data (filled squares). C–bearing features are labeled by vertical solid lines, while O–bearing ones are labeled by vertical dotted lines.

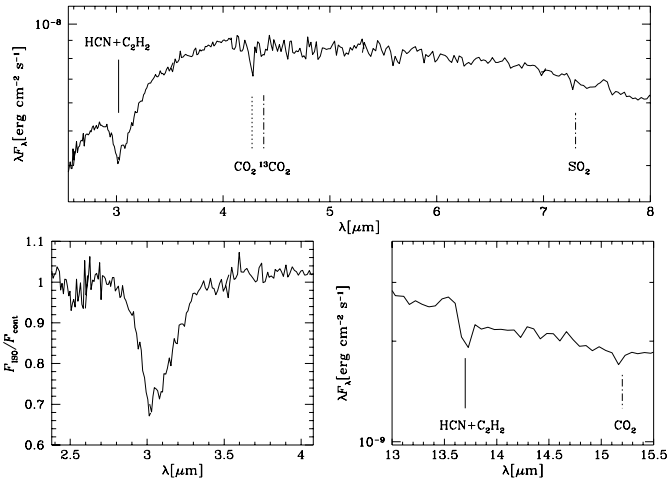

Fig. 2. The spectral features in ISO–SWS spectrum of IRAS 03201+5459 with their identifications. C–bearing features at 3 μm and 13.7 μm of C_2H_2 and HCN are labeled by solid lines and the O–bearing feature at 4.27 μm of molecule CO_2 is labeled by a dashed line. Tentative detections at 4.38 μm of $^{13}CO_2$, at 7.3 μm of SO_2 and at about 15.2 μm of CO_2 are marked by dot–dashed lines. Lower left panel shows a continuum–divided spectrum around 3 μm.

3. Discussion

3.1. Spectral features

The spectrum shown in Fig. 1 exhibits many features. Some of them are weak or blended and their identifications are uncertain. However, some features are relatively strong and isolated from other lines. The last include absorption features at 4.27 and 13.68 μm, a broad emission band around 18.1 μm (which, however, most likely is an artifact produced by the glitches – see below), and the other two broad absorption bands at 3.02 and 9.7 μm. To see these and other tentative detections in more detail part of the SWS spectrum is enlarged in Fig. 2 where, for sake of comparison, a continuum–divided spectrum around 3 μm is shown in the lower left panel.

The suggestion of C–richness of IRAS 03201 comes from its absorption feature around 3.0 μm. Systematic spectrophotometric observation of cool stars in the 2–4 μm region by Merrill & Stein (1976a, 1976b) and Noguchi et al. (1977) revealed this feature in all the observed carbon stars. Furthermore, Ridgway

et al. (1978) identified the absorption features around 3.0 μm in spectra of carbon stars as different bands of C_2H_2 and HCN molecules (see also Cernicharo et al. 1999 for the most recent ISO results). This feature is thus a strong indication of C–richness. The comparison of 3.0 μm band of IRAS 03201 with that of genuine C–rich star IRC+10216 (Cernicharo et al. 1999) shows them to be similar in shape and position, while there are significant differences with the 3.0 μm water ice band observed in O–rich stars (e.g. Sylvester et al. 1999). The 3.0 μm band consists of two absorption valleys whose minima are at about 3.02 and 3.08 μm and the first one being deeper if it is due to C–bearing molecules and is relatively irregular with predominantly single minimum at about 3.05–3.10 μm if it is due to water ice. The idea that the 3 μm feature in IRAS 03201+5459 is C–based is further supported by the existence of another feature at about 13.7 μm which is detected in the ISO–SWS spectra of several C–rich stars (Yamamura et al. 1998) and interpreted as a ν_5 band of C_2H_2 molecule. More detailed comparison of the 3.0 μm band between IRAS 03201 and IRC+10216 revealed that the IRAS 03201 band is wider with its wings extending from about 2.8 up to 3.3 μm (see the lower left panel of Fig. 2), and slightly stronger relative to the continuum than that of IRC+10216. In order to fit the wings Cernicharo et al. (1999) introduced a contribution from warm gas near the star which is probably related to stellar pulsations (Woitke et al. 1999). The broader wings of the 3.0 μm feature then suggest that the excitation temperature in the case of IRAS 03201 is higher.

On the other hand, in the SWS 01 spectrum of IRAS 03201 there are a few features which usually occur in an O–rich environment. The broad absorption feature at 9.7 μm is generally accepted as a stretching band of amorphous silicate dust. It is seen in O–rich AGB stars with optically thick circumstellar shells. Because the oxygen atoms are thought to react effectively with carbon to form CO, there is no excess of oxygen atoms to generate silicates in a C–rich environment. As can be seen from the following model fitting, the center of this feature actually is a little blue shifted (exact center at 9.67 μm) in comparison with that expected from the *circumstellar* silicates (David & Pegourie 1995). It could mean that this band is due to some polluted silicate dust other than the *circumstellar* silicates. Therefore the possibility mentioned in the Introduction that the observed feature could be due to interstellar absorption is investigated here in more detail. Detailed maps in ^{12}CO (Digel et al. 1996) showed that there is an intervening cloud in direction of our source (l = 143.59°, b = −1.46°) which has a peak of ^{12}CO emission at l = 143.8° and b = −1.5° and a line–of–sight velocity with respect to the local standard of rest, $V_{\rm LSR}$, about $-30\,{\rm km\,s^{-1}}$. This cloud (no. 59 in Table 3 of Digel et al. (1996)) could be physically related to the BFS31–H II region in the Perseus arm. The same region of the sky has been surveyed at ^{13}CO by Obayashi et al. (1999). Observing at l = 143.6° and b = −1.47° with the beam size of 2.7 arcmin they detected weak emission, from which the estimated column density of ^{13}CO is $3.3\,10^{15}\,{\rm cm^{-2}}$ and $V_{\rm LSR} = -25.9\,{\rm km\,s^{-1}}$. Using the relation between ^{13}CO column density and visual extinction, $A_{\rm V}$, derived for the Perseus complex by Bachiller & Cernicharo (1986), we estimated that $1.5 < A_{\rm V} < 3.0$ for the molecular cloud in the line–of–sight towards the investigated source. The spectrum of IRAS 03201 corrected for interstellar extinction following the law of Rieke & Lebofsky (1985) with $A_{\rm V} = 3$ is shown as a dotted line in Fig. 3. As it can be seen the estimated absorption by interstellar silicates hardly accounts for the observed 9.7 μm feature in the IRAS 03201 spectrum. Note that after such correction for interstellar extinction we have found a more pronounced signature of SiC at 11.3 μm, which suggest again that IRAS 03201 is a genuine carbon star. Under Rieke & Lebofsky (1985) extinction law the silicate absorption feature would disappear when $A_{\rm V}$ is between 7 and 8 mag. However, if the extinction law of Mathis (1990) is applied then the required $A_{\rm V}$ would be about 11 mag. Such an $A_{\rm V}$ is a factor of 3 or even more larger than the value inferred from the ^{13}CO observations.

There are at least four possible explanations of this discrepancy. Firstly, the relation of Bachiller & Cernicharo (1986) between ^{13}CO column density and $A_{\rm V}$ for the Perseus complex could be invalid in this specific direction. However, we have checked that such relations derived for other molecular complexes (Harjunpää & Mattila 1996) neither predict an $A_{\rm V}$ big enough to account for the observed strength of 9.7 μm feature. For a ^{13}CO column density of about $3.3\,10^{15}\,{\rm cm^{-2}}$ the largest derived value of $A_{\rm V}$ is about 4.6 mag, obtained using the relation for the Coalsack local cloud. Secondly, the beam size of the ^{13}CO observations (2.7 arcmin) is relatively large and it is possible that the column density averaged through this field of view is underestimated in the direction of this object. Only further observation with a smaller beam size could help resolve this problem. Thirdly, the extinction law in the direction of IRAS 03201 could be unusual (much larger $A_\lambda/A_{\rm V}$ than in the extinction law of Rieke & Lebofsky (1985) or Mathis (1990)). To check this possibility it would be necessary to perform an interstellar extinction law determination for stars located close to the line–of–sight towards IRAS 03201. In summary, we conclude that presently available observations cannot explain the strength of 9.7 μm absorption feature solely by interstellar silicates. In addition, the extinction maps of Neckel & Klare (1980) suggest that $A_{\rm V}$ is only about 2 for a distance up to about 4 kpc in a relatively large field which covers the location of IRAS 03201 (see their Figs. 5b and 6b 31(144-3)). Therefore, it seems plausible to consider the fourth explanation. Namely, that some of the absorbing silicates are related to the star itself and located in an outer O–rich shell or stored in more disk–like configuration (see Sect. 3.2).

Observations of dust in interstellar medium show that the structure of silicates remains mostly amorphous (Dorschner & Henning 1995). However, crystalline silicates are present in significant amounts around some late type stars including post–AGB sources and planetary nebulae (Waters et al. 1998a, Waters et al. 1998b, Cohen et al. 1999, Waters & Molster 1999, Molster et al. 1999b). Spectroscopic observations (Waters & Molser 1999) seem to suggest that crystalline silicates tend to appear only when the mass loss rate from the star is sufficiently high. These data also suggest that the process of crystallization takes

place not only in the long–lived reservoir of orbiting matter left over from previous episodes of mass loss (e.g. the Red Rectangle – Waters et al. 1998a) but also in the outflows from late type stars (e.g. OH 32.8-0.3 – Waters & Molster 1999). Therefore the presence of crystalline silicate bands in our SWS 01 spectrum would suggest the existence of oxygen rich material concentrated around IRAS 03201. In spite of poor data quality in band 3, features of crystalline enstatite and/or forsterite at 21.5, 24.5 and relatively strong emission at about 18.1 μm seem to be present. For comparison, in Fig. 1 we have marked some positions (16.1, 18.1, 21.5, 23.6 and 24.5 μm) of crystalline silicate bands identified in the spectrum of AFGL 4106 by Molster et al. (1999a). Because the strength and shape of the 18.1 μm feature is rather unusual as compared to the already published ISO spectra with crystalline silicate signatures, we examined carefully the data from all detectors in band 3C. We found that there are two glitches: one at about 17.5 μm in the down scan (increasing wavelength with time of observation) and a second at about 18.5 μm in the up scan (decreasing wavelength). The extended tails which result from these glitches overlap (the down scan is particularly disturbed by this) and it is very difficult to find the continuum in the vicinity of 18 μm. Therefore, we think that the feature seen around 18.1 μm is most likely an artifact of data reduction. A small contribution from crystalline silicates could be present but it is impossible to prove this on the basis of our ISO data.

In ISO SWS 01 spectrum of IRAS 03201, there is another O–bearing molecular absorption feature at 4.27 μm, identified as due to solid CO_2. The identification is furthermore supported by the tentative detection of an absorption around 15.2 μm also due to solid CO_2, and a tentatively detected absorption at 4.38 μm from solid $^{13}CO_2$ (see Fig. 2). The narrowness of the feature with minimum around 4.27 μm suggests it is caused by polar (H_2O and/or CH_3OH–rich) CO_2 ice (e.g. Ehrenfreund et al. 1999) while the wing on the short wavelength side of this feature is probably due to a non-polar component (e.g. Sandford & Allamandola 1990). Most likely, the CO_2 ice bands in spectrum of IRAS 03201 come from the intervening cloud discussed above. The column density, N(CO_2) (assuming band strength $7.8\,10^{-17}$ cm molecule^{-1} – Gerakines et al. 1995) is only about $4\,10^{16}$ cm^{-2}, one of the smallest values found (see e.g. Table 7 of Gerakines et al. 1999). This could favour the explanation that the intervening cloud is not of high A_V. The column density determination for $^{13}CO_2$ is very uncertain since the feature at 4.38 μm is weak and the spectrum around it is noisy. However under the resolution and signal to noise ratio achieved in the case of IRAS 03201, we cannot conclude that solid and/or gaseous CO_2 does not exist around the source itself. For example, relatively broad absorption feature around 4.2–4.3 μm and weak absorption around 14.97 μm have been detected the Red Rectangle, a C–rich object, (Waters et al. 1998a) and attributed to gas–phase CO_2, although as they state the contribution from solid CO_2 of circumstellar origin to the 4.27 μm band is also possible. The stretching–mode resonance of gaseous CO_2 visible in range from about 4.20 to 4.35 μm with minimum around 4.23 μm has been detected in the O–rich star NML Cyg (Justtanont et al. 1996), in two O–rich Miras (Yamamura et al. 1999b) and in a few OH/IR stars (Sylvester et al. 1999).

One more example of O–bearing molecular features in our spectrum is the tentatively detected absorption feature around 7.3 μm due to the ν_3 band of SO_2, discovered in O–rich Miras by Yamamura et al. (1999a). However, it is also possible that the overall structure in 7–8 μm range is due to the C_2H_2 $\nu_4 + \nu_5$ bands (Aoki et al. 1999). Because of relatively low quality of data in this part of the spectrum, we are not sure of the nature of this feature.

Summarizing above discussion all the O–based features detected in the spectrum of IRAS 03201 could be, at least partly, of interstellar origin. However, we were not able to prove that the interstellar extinction is high enough to be responsible for the observed strength of the 9.7 μm absorption feature. Therefore, it seems plausible to consider that at least part of the O–rich features are of circumstellar origin. The co–existence of both O–bearing and C–bearing spectral features would suggest that the object is chemically complex. An alternative possibility is that the C–bearing molecules are produced at the outer ($R > 10^{16}$ cm) part of the O–rich envelope due to UV dissociation of molecules and succeeding chemical reactions. In fact, HCN and HCO^+ have been detected in O–rich late-type stars (Deguchi & Goldsmith 1985, Morris et al. 1987). However, the molecules lying at the outer part of the envelope are usually cold and cannot produce the wide absorption band at 3.0μm as seen in the spectrum of IRAS 03201.

3.2. Spectral energy distribution

In order to investigate the nature of this object, we try to fit the spectral energy distribution (SED) by radiative transfer modelling. Without additional observations we are not able to solve the question of the location of O–rich material, i.e. whether this material is located in some kind of disk–like structure seen edge on or it is flowing outwards after a phase of O–rich mass loss. For the purpose of this paper we will consider only the later possibility.

The basic idea of such a model is a solution of the radiative transfer through the dusty circumstellar envelope. The central star is assumed to radiate as a blackbody and to lose mass at constant rate with the resulting envelope expanding at constant velocity. Under these assumptions, the frequency–dependent radiative transfer equations are solved under the spherically–symmetric geometry simultaneously with the thermal balance equation for dust (Szczerba et al. 1997). The important parameters that determine the final SED include the properties of the star, the properties of the gas/dust envelope and the (dust) mass loss rate. They are adjusted in a reasonable range for an AGB star in order to fit the observed SED. Because no information is available on the expansion velocity of the circumstellar envelope, a typical value of 15 km s^{-1} is adopted. As a first step, a one–dust–component model is constructed in spite of the conflicting circumstellar spectral features.

No reasonable fit to the SED could be found by assuming circumstellar silicates (David & Pegourie 1995) as the dust com-

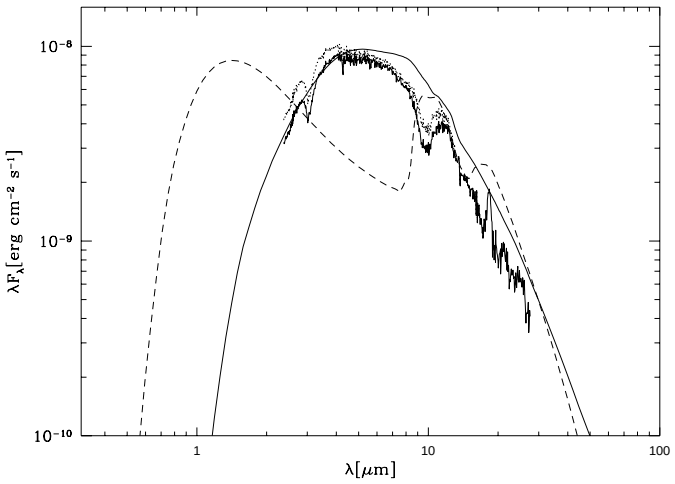

Fig. 3. The AC1 dust model fit to the SED. The solid line represents the model fitting whose parameter values are listed in Table 1. For comparison, the output from a silicate dust model using the same parameters is over-plotted as the dashed line. The AC1 dust model produces narrower SED than does the silicate dust model, which approximates the observed SED much better. The observed spectrum is shown by thin solid line for data without correction for interstellar extinction and by dotted line for data with correction for interstellar extinction with A_V = 3.0.

Table 1. Parameters for AC1 dust model.

parameter	value
$T_{\rm eff}$	3000 K
$L_{\rm star}$	8000 $L_\odot$
d	4.1 kpc
$T_{\rm inn}$	800 K
$R_{\rm inn}$	4.1 10^{14} cm
$R_{\rm out}$	1.0 10^{16} cm
$t_{\rm dyn}$	2.11 10^2 yr
$\dot{M}$	1.0 10^{-5} $M_\odot$/yr
Dust–to–gas ratio	5.0 10^{-3}
a_-	0.005 μm
a_+	0.25 μm
p (power–law index of size dist.)	3.5
A_V	18.0

ponent in the circumstellar envelope, even when the parameters for the model were changed over a wide range. The main shortcoming of the silicate dust model lies in its producing too wide an SED in comparison with the observed SED of IRAS 03201. On the other hand, a reasonable fit to the continuum radiation is achieved by assuming amorphous carbon (AC1 from Rouleau & Martin 1991) as the dust component of the circumstellar envelope. The values of key parameters for the best fit with AC1 are listed in Table 1. The stellar effective temperature 3000 K and luminosity 8000 $L_\odot$ are typical of a late C–type star, with the derived distance of 4.1 kpc being dependent on the actual luminosity. The mass loss rate of $10^{-5}\,M_\odot\,{\rm yr}^{-1}$ is relatively high; it is determined from the dust mass loss rate through the dust–to–gas ratio assumed to be $5.0\,10^{-3}$. The dust size distribution is assumed to be a power–law function of the dust grain radius. This set of parameters describes a C–rich AGB star with relatively large mass loss rate and a cold circumstellar envelope. The resulting fit is shown in Fig. 3 by the solid line. Except for excess emission in the 5–10 μm range, the model approximates the observed SED. For comparison, the result for the same set of parameters except with the dust component replaced by circumstellar silicates is over-plotted in Fig. 3 as the dashed line. The difference in the opacity properties of silicate and AC1 dust is such that the former one cannot fit the observed spectrum in the case of IRAS 03201. The AC1 dust transfers the optical radiation of the central star to 2–10 μm much more efficiently and to long wavelengths beyond 10 μm much less efficiently than does the silicate dust, which results in a narrower SED. This suggests that there must be some C–rich dust around IRAS 03201.

3.3. Two–dust–component model

According to the theoretical study of stellar evolution in the AGB phase, when a carbon star forms there should be a period when the star has two dust components in the circumstellar envelope. When the third dredge–up process occurs, the newly produced carbon and other elements from the He–burning shell are convected to the surface of the stellar photosphere, which can then be brought to the circumstellar envelope by a stellar wind. When the O–rich star becomes C–rich after the *fatal* He–shell flash, both sorts of dust could co–exist in the circumstellar envelope. This phase is short (of order of hundred years – see e.g. Mowlavi 1999) and thus difficult to catch observationally, but, at least theoretically it is not impossible to find such object.

We constructed a model based on such a theoretical scenario with a central star surrounded by an inner C–rich and an outer O–rich circumstellar shell. We assume that there is no gap between the two shells, which means the mass loss is continuous when the star changes chemical composition. The earlier mass loss process forms the outer O–rich shell and the later mass loss after the star becomes C–rich creates the inner C–rich shell. The basic framework of the model is then similar to that for one dust component, i.e. the frequency–dependent radiative transfer equations are solved under the spherically–symmetric geometry simultaneously with the thermal balance equation for a dusty envelope. As the mass loss rate and dust–to–gas ratio are dependent on each other, the mass loss rate is assumed to be the same for these two phases of mass loss process but the dust–to–gas ratios can differ.

The best fit we can obtain by the two–dust model is an improvement in comparison with the one–dust component model. Both the silicate feature and the overall energy distribution can be approximately fit simultaneously. The values of key parameters for this fit shown in Fig. 4 are listed in Table 2. If the dust–to–gas ratios for O–rich and C–rich stellar winds are the same then the O–rich mass loss rate would be 1.6 times that for C–rich case. The thinner C–rich shell close to the central star extends up to about 0.15 $R_{\rm out}$ and the geometrically thicker O–rich shell is located in the outer part. The expansion velocity is assumed to be 15 km s^{-1} and to be the same for the two types of

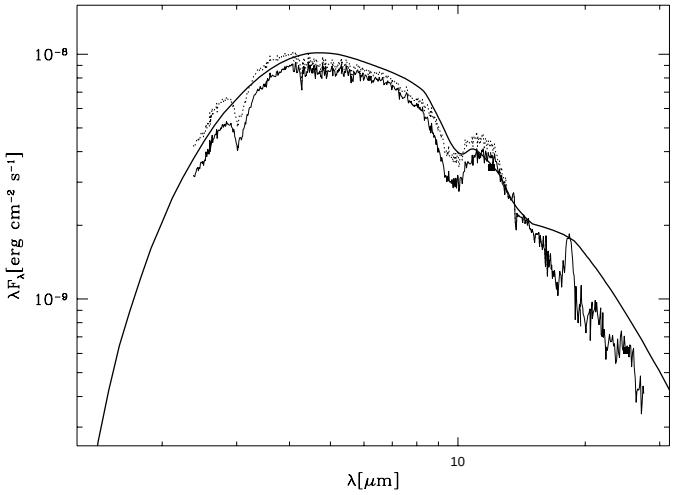

Fig. 4. The two dust model fit to the SED. The circumstellar shell is assumed to be composed of an inner C–rich shell of AC1 dust and an outer O–rich shell of silicate dust. The solid line represents the model fitting whose parameter values are listed in Table 2. The observed spectrum is shown by thin solid line for data without correction for interstellar extinction and by dotted line for data with correction for interstellar extinction with A_V = 3.0.

Table 2. Key parameters for two–dust (AC1+silicate) model

Parameter	Value
$T_{\rm eff}$	2800 K
$L_{\rm star}$	8000 $L_\odot$
d	4.2 kpc
$T_{\rm inn}$	800 K
$R_{\rm inn}$	4.2 10^{14} cm
$R_{\rm out}$	1.0 10^{16} cm
$t_{\rm dyn}$	2.11 10^2 yr
$R_{\rm AC1shell}$	0.06–0.15 $R_{\rm out}$
$R_{\rm silicateshell}$	0.15–1.00 $R_{\rm out}$
$\dot{M}$	1.1 10^{-5} $M_\odot$/yr
Dust–to–gas ratio (AC1 shell)	5.0 10^{-3}
Dust–to–gas ratio (silicate shell)	8.0 10^{-3}
A_V	21.6

circumstellar shells so that the ages of the two shells are 31 yrs and 180 yrs, respectively. In other words, the model implies that the C–rich stellar wind started 31 years ago if the expansion velocity is 15 km s^{-1} or about 50 years ago if $V_{\rm exp}$ = 10 km s^{-1}, and that the O–rich stellar wind started 211 years if $V_{\rm exp}$ = 15 or about 300 years ago if $V_{\rm exp}$ = 10 km s^{-1}. The end of the O–rich wind and the start of C–rich wind occurred in our model at the same time. The time seems short for the O–rich mass loss process. Increasing the outer radius of the model would result in a longer duration of the O–rich mass loss phase although the far–infrared radiation would increase at the same time if the density distribution remains the same. A possible explanation is that the density distribution of the O–rich shell decreases more steeply with radius than the assumed power law with index -2 (which would correspond to increasing mass loss rate with time). A more steeply decreasing distribution of the density of the shell would enlarge the outer radius of the shell while keeping the far–infrared radiation almost unchanged. Another possibility is that the O-rich shell is located far away from the star (Rowan-Robinson 1982) which would give a better fit in the FIR band, but which requires a large amount of mass, which is in conflict with the AGB nature (C-richness) of the object.

Early in 1986, Little–Marenin (1986) and Willems & de Jong (1986) found nine stars which showed silicate emission at 9.7 μm but were optically identified as carbon stars. Some of these sources may be mis–identified, but several others do seem to have both the silicate and C–rich features (see e.g. Kwok et al. 1997 for one of the most recent lists of such sources). Because the majority of these silicate carbon stars are ^{13}C–enhanced J–type (Lambert et al. 1990, Le Bertre et al. 1990, Lloyd–Evans 1990), a binary model was proposed. However the presence of a mass–losing O–rich companion was ruled out observationally for a number of silicate carbon stars (Noguchi et al. 1990; Engels & Leinert 1994). In addition, an object with both O–rich and C–rich spectral features has been found in LMC (Trams et al. 1999). In a single–star model, such silicate carbon stars would have experienced O–rich mass loss which formed the O–rich shell that has already expanded to become optically thin at 9.7 μm, producing the emission feature. Their central stars have become C–rich after the third dredge–up process ejected the freshly produced C from the burning shell to the photosphere. Note, however, that Jura & Kahane (1999) found narrow emission lines of CO from two carbon–stars with oxygen–rich envelopes, which can be interpreted as an evidence of long–lived reservoir of orbiting gas in a thin disk. This gas, if O–rich and not seen exactly edge–on, could give rise to observed silicate emission.

Despite the still ongoing discussion on the nature of silicate carbon–stars, IRAS 03201+5459 might be related to this group of sources. As opposed to previously known sources, the feature at 9.7 μm is in absorption rather than in emission. That would mean the O–rich shell is still optically thick at 9.7 μm, if we follow the outflow scenario the object is at earlier evolutionary stage than those with an emission feature at 9.7 μm. Willems & de Jong (1986) suggested that after the transition from O–rich to C–rich star there is an interruption of mass loss. Investigation of the chemical composition inside detached shells by Zuckerman (1993) suggested, however, that such shells could be C–rich rather than O–rich. The short timescales for O–rich and C–rich shells derived from the modelling of SED for IRAS 03201 could be interpreted as a signature of the mass loss during the ongoing thermal pulse. After the transformation of the atmosphere from O–rich to C–rich the dust composition changes correspondingly and the mass loss follows the luminosity behaviour during the thermal pulse. If so, then in a short time the mass loss rate would decrease significantly and the already C–rich star in IRAS 03201 might appear as an object with silicate emission and then as an optically identified C–star with a detached shell and with no clear signature of O–richness inside the expanding shell (see example of theoretical modelling of the AGB evolution by Steffen et al. 1998). Taking into account the obtained circumstellar A_V of about 20 and the expansion velocity of 15 km s^{-1} we can

estimate that it would take no longer than 300 years until the circumstellar envelope of IRAS 03201 becomes optically thin. Whether the source would become a silicate carbon–star with 9.7 μm feature in emission or not is a matter of dust temperature inside O–rich shell at that moment. The puzzling point of our model is the short time we deduce since the star became carbon–rich (about 50 years). In such a case the 14 year gap between the IRAS and ISO observations should probably produce some change in the infrared spectrum of newly created C–star. In spite of the low IRAS LRS data quality (cf. Fig. 1) we can see that there is no significant difference between the IRAS LRS and ISO SWS spectra.

3.4. Other possibilities

There could be an alternative scenario related to the nature of IRAS 03201. The broad features at 3 μm and 9.7 μm are seen simultaneously in the so–called BN Orion objects (Merrill & Stein 1976c, Willner et al. 1982). Such objects represent a very early stage of stellar evolution (Becklin & Neugebauer 1968) and are referred to protostars. The 3 μm feature in protostars is attributed to amorphous water ices (Gillet & Forrest 1973) and the 9.7 μm feature is attributed to the silicate particles as in the late–type O–rich stars. The spectrum of the protostellar object RAFGL 7009S by ISO–SWS in AOT 01 mode revealed the absorption features of CO_2 at 4.27 μm and 15.21 μm (Ehrenfreund et al. 1997). So apparently all the strong spectral features present in IRAS 03201 can be explained if it is a protostar. However, the 3 μm feature observed in IRAS 03201 resembles that produced by C_2H_2 and HCN molecules in C–type stars instead of that of water ice in protostars. The SED does not support the protostar model either. The 2–10 μm region of SED can be fit roughly by a blackbody at a temperature of about 760 K which gives a little less emission in the longer wavelength than the observed spectrum. The blackbody–like SED is consistent with the characteristics of protostars, but this temperature is too high for protostars.

One more possible explanation of IRAS 03201 nature is related to the fact that the spectral energy distribution of IRAS 03201 looks similar to that of late–type Galactic Wolf–Rayet (WR) stars (e.g. van der Hucht et al. 1996). In this group of objects the observed 9.7μm features are solely interpreted as due to the interstellar absorption. However, there are many differences between IRAS 03201 and the galactic Wolf–Rayet stars. For example, neither the 3.0 μm feature nor the CO_2 absorption features have been detected in any of the WR stars.

4. Conclusions

We have investigated the nature of IRAS 03201+5459 by analysis of its near– and mid–IR spectrum covering 2.3 to 45 μm using a full grating scan taken with the SWS spectrometer on board of ISO with the second fastest speed. The obtained spectrum shows the features of both C–based molecules (at 3.02 and 13.07 μm attributed to the transitions in HCN and/or C_2H_2) and O–based ones (at 9.7 μm related to amorphous silicates and at 4.27 μm caused by solid CO_2). The broad feature at 3.02 μm can be explained only if HCN and/or C_2H_2 molecules are formed near the stellar surface, making the star genuinely carbon–rich. However, just from the SWS 01 spectrum we cannot solve the puzzle of the location of O–rich material: whether it is only of interstellar origin, or freely flowing out of the star or more confined to some disk–like configuration. Without further observations we can not completely exclude a possibility that A_V to this object is underestimated and/or the interstellar extinction law in the direction of our source is unusual and, in consequence, that 9.7 μm band is solely of interstellar origin. However, at the moment, we are not able to fully explain the 9.7 μm absorption by interstellar matter and we have considered the hypothesis that IRAS 03201+5459 is presently a carbon-rich AGB star which is experiencing or has recently experienced the *fatal* thermal pulse that changed the star chemistry. In principle, our numerical radiative transfer modelling shows that it is possible to explain the complex nature of IRAS 03201 on the basis of an outflow model in which a still optically thick O–rich envelope is followed by the newly created C–rich one. Nevertheless this model has difficulty explaining the similarity between the IRAS and ISO spectra, since it implies a very recent transition of the star into a carbon star. It is possible that the O–rich material is located in some disk–like configuration around IRAS 03201 so that it can be stable for long periods of time, but only careful investigation of the molecular cloud in the line–of–sight of IRAS 03201+5459 could solve this puzzle.

Acknowledgements. Authors thank Dr. A. Obayashi for providing with details her observations before publication. They also express their gratitude to Dr. Kevin Volk for his careful reading of the manuscript and useful suggestions. This work has been partly supported by grant 2.P03D.002.13 of the Polish State Committee for Scientific Research and by the International Collaboration Bureau of Chinese Academy of Sciences. R Sz acknowledges also support from the JSPS Invitation Fellowship Program for Research in Japan.

References

Aoki W., Tsuji T., Ohnaka K., 1999, A&A 350, 945
Bachiller R., Cernicharo J., 1986, A&A 166, 283
Becklin E., Neugebauer G., 1968, ApJ 147, 799
Cernicharo J., Yamamura I., Gonzalez–Alfonso E., et al., 1999, ApJ 526, L41
Cohen M., Barlow M.J., Sylvester R.J., et al. 1999, ApJ 513, L135
David P., Pegourie B., 1995, A&A 293, 833
de Graauw Th., Haser L., Beintema D., et al., 1996, A&A 315, L345
Deguchi S., Goldsmith P.F., 1985, Nat 317, 336
Digel S.W., Lyder D.A., Philbrick A.J., et al., 1996, ApJ 458, 561
Dorschner J., Henning Th., 1995, A&AR 6, 271
Ehrenfreund P., Boogert P.A., Gerakines W.A., et al., 1997, Icarus 130, 1
Ehrenfreund P., Kerkhof O., Schutte W.A., et al., 1999, A&A 350, 240
Engels D., Leinert C., 1994, A&A 282, 858
Galt J., Kwok S., Frankow J., 1989, AJ 98, 2182
Gerakines P.A., Schutte W.A., Greenberg J.M., et al., 1995, A&A 296, 810
Gerakines P.A., Whittet D.C.B., Ehrenfreund P., et al., 1999, ApJ 522, 357

Gillett F., Forrest W., 1973, ApJ 179, 483
Harjunpää P., Mattila K., 1996, A&A 305, 920
IRAS Point Source Catalog, Version 2, 1988, Joint IRAS Science Working Group, Washington, DC (PSC)
Jiang B.W., Hu J.Y., 1992, Chin. A&A 16, 416
Jiang B.W., Deguchi S., Yamamura I., et al., 1996, ApJS 106, 463
Jura M., Kahane C., 1999, ApJ 521, 302
Justtanont K., de Jong T., Helmich F.P., et al., 1996, A&A 315, L217
Kwok S., Volk K., Bidelman W.P., 1997, ApJS 112, 557
Lambert D., Hinkle K., Smith V., 1990, AJ 99, 1612
Le Bertre T., Deguchi S., Nakada Y., 1990, A&A 235, L5
Little–Marenin I.R., 1986, ApJ 307, L15
Lloyd–Evans T., 1990, MN 243, 336
Mathis J.S., 1990, ARA&A 28, 37
Merrill K., Stein W., 1976a, PASP 88, 285
Merrill K., Stein W., 1976b, PASP 88, 294
Merrill K., Stein W., 1976c, PASP 88, 874
Molster F.J., Waters L.B.F.M., Trams N.R., et al., 1999a, A&A 350, 163
Molster F.J., Yamamura I., Waters L.B.F.M., et al., 1999b, Nat 401, 563
Morris M., Guilloteau S., Lucas R., et al., 1987, ApJ 321, 888
Mowlavi N., 1999, In: Le Bertre T., Lèbre A., Waelkens C. (eds.) Proceedings of the IAU Symp. 191, ASP, p. 47
Neckel Th., Klare G., 1980, A&AS 42, 251
Noguchi K., Maihara T., Okuda H., et al., 1977, PASJ 29, 511
Noguchi K., Murakami H., Matsuo H., et al., 1990, PASJ 42, 441
Obayashi A., Yonekura Y., Mizuno A., et al., 1999, In: Nakamoto T. (ed.) Proceedings of the International Conference. The Nobeyama Radio Observatory, p. 84
Olnon F.M., Raimond E., Neugebauer G., et al., 1986, A&AS 65, 607
Rieke G.H., Lebofsky M.J., 1985, ApJ 288, 618
Ridgway S.T., Carbon D.F., Hall D.N.B., 1978, ApJ 225, 138
Rouleau F., Martin P.G., 1991, ApJ 377, 526
Rowan-Robinson M., 1982, MNRAS 201, 281
Sandford S.A., Allamandola L.J., 1990, ApJ 355, 357
Steffen M., Szczerba R., Schönberner D., 1998, A&A 337, 149
Szczerba R., Omont A., Volk K., et al., 1997, A&A 317, 859
Sylvester R.J., Kemper F., Barlow M.J., et al., 1999, A&A 352, 587
Trams R., van Loon J., Zijlstra A., et al., 1999, A&A 344, L17
van der Hucht K.A., Morris P.W., Williams P.M., et al., 1996, A&A 315, L193
van der Veen W.E.C.J., Habing H.J., 1988, A&A 194, 125
Volk K., Cohen M., 1989, AJ 98, 931
Waters L.B.F.M., Waelkens C., van Winckel, et al., 1998a, Nat 391, 868
Waters L.B.F.M., Beintema D.A., Zijlstra A.A., et al. 1998b, A&A 331, L61
Waters L.B.F.M., Molster F.J., 1999, In: Le Bertre T., L'ebre A., Waelkens C. (eds.) Proceedings of the IAU Symp. 191, ASP, p. 209
Willems F., de Jong T., 1986, ApJ 309, L39
Willner S., Gillet F.C., Herter T.L., et al., 1982, ApJ 253, 174
Woitke P., Helling Ch., Winters J.M., et al., 1999, A&A 348, L17
Yamamura I., de Jong T., Justtanont K., et al., 1998, Ap&SS 255, 351
Yamamura I., de Jong T., Onaka T., et al., 1999a, A&A 341, L9
Yamamura I., de Jong T., Cami J., 1999b, A&A 348, L55
Zuckerman B., 1993, A&A 276, 367
Zuckerman B., Lo K., 1987, A&A 173, 263